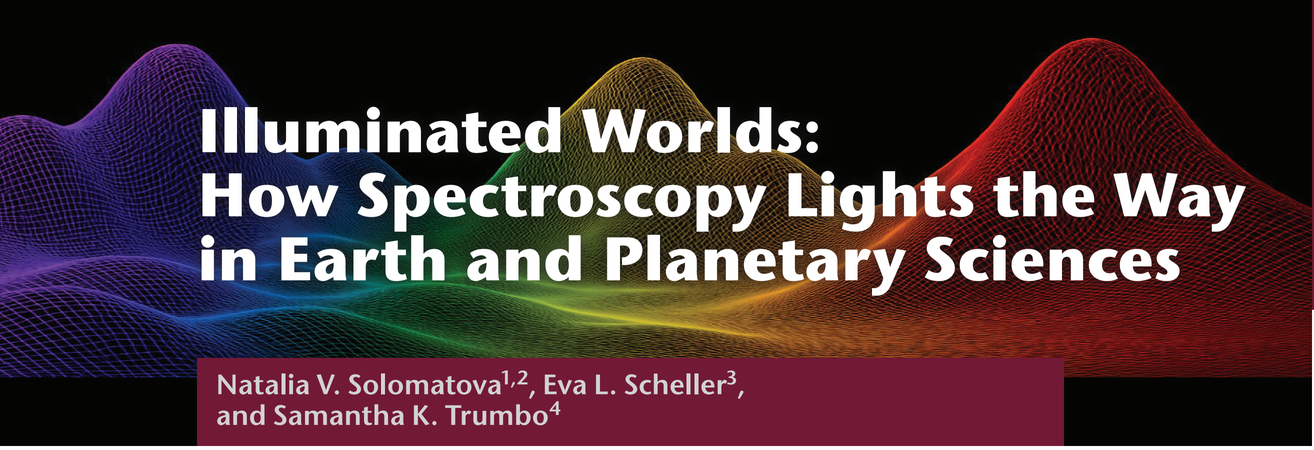

Illuminated Worlds: How Spectroscopy Lights the Way in Earth and Planetary Sciences

Natalia V. Solomatova[1,2], Eva L. Scheller[3], and Samantha K. Trumbo[4]

The graphical banner is an artistic depiction of the visible light spectrum in the context of mineralogy and planetary science, and was generated using OpenAI.

1811-5209/26/0022-082$2.50 DOI: 10.2138/gselements.22.2.82

The study of minerals under light, spanning the ultraviolet, visible, infrared (UV-Vis-IR) spectrum, has played an important role in advancing our understanding of terrestrial and extraterrestrial materials. Here, we review light-based spectroscopic techniques across spatial scales in mineralogy and planetary science. Polarized light microscopy helps characterize optical properties, while vibrational and UV-Vis spectroscopies provide insights into mineral structures and compositions. In mineral physics, spectroscopy probes bonding environments, electronic structure, phase transitions, and elastic properties at high pressures and temperatures. In planetary science, UV-Vis-IR techniques from spacecraft and telescopes reveal planetary mineralogy. These methods support the search for habitable environments, planetary evolution studies, and resource identification. Furthermore, technological advances in portability, imaging, and data analysis have improved the precision and scope of mineralogical research.

KEYWORDS: spectroscopy; mineralogy; planetary science; geochemistry; vibrational spectroscopy; hyperspectral imaging

INTRODUCTION

Light-based spectroscopy, here defined as spanning the ultraviolet, visible, and infrared (UV-Vis-IR) regions of the **electromagnetic spectrum***, is widely used to identify and characterize minerals across Earth, environmental, and planetary sciences. Techniques such as optical microscopy, UV-Vis-NIR (near-infrared) spectroscopy, **Fourier-transform infrared (FTIR) spectroscopy**, **Raman spectroscopy**, and orbital imaging spectroscopy allow researchers to probe the structural, physical, chemical, and electronic properties of minerals based on how they interact with light. As illustrated in FIGURE 1, these methods range from laboratory analyses of micrometer-scale grains, to thin-section petrography, to field and drone-based measurements, and ultimately to airborne and satellite observations covering regional to planetary extents. This manuscript reviews these techniques with emphasis on their underlying physical principles, instrumentation, and mineral physics applications, providing readers with a foundation in light-based mineral characterization.

1 Miraterra Technologies
Vancouver, V5Y1K3, BC, Canada
E-mail: natalia.solomatova@miraterrasoil.com

2 Arca Climate Technologies
Vancouver, V5Y1M8, BC, Canada

3 Stanford University
Stanford, CA 94305, USA
E-mail: eschelle@stanford.edu

4 University of California San Diego
San Diego, CA 92093, USA
E-mail: sktrumbo@ucsd.edu

MINERALS UP CLOSE: LAB-BASED SPECTROSCOPY AND MICROSCOPY

Bonds and Bands: Vibrational Spectroscopy of Minerals

At the smallest spatial scales considered here, vibrational techniques such as Fourier transform infrared (FTIR) and Raman spectroscopy probe lattice and molecular vibrations, providing information on bonding environments, coordination, and crystal structure. When light interacts with a mineral, it can couple to the natural vibrational frequencies of chemical bonds and crystal lattices. These vibrations represent collective motions of atoms, such as stretching or bending of bonds within the structure. A vibrational mode is IR active if it involves a change in **dipole moment** during the vibration, meaning that the distribution of electrical charge within the bond oscillates as the atoms move. In contrast, a vibrational mode is Raman active if it involves a change in **polarizability**, that is, if the electron cloud can be distorted more or less easily as the atoms vibrate. In centrosymmetric structures, many modes are either IR active or Raman active, but not both, whereas in lower-symmetry structures, some modes satisfy both criteria. This difference explains why FTIR and Raman spectra often contain complementary sets of peaks. Together, these methods are used from micron-scale grains and inclusions to bulk materials (King and Mernagh 2024).

FTIR methods identify functional groups and structural units such as Si-O stretching in silicates, CO_3^{2-} stretching in carbonates, and OH bands in hydrous minerals. Conventional transmission measurements use powders mixed with KBr and pressed into pellets or formed into thin films. ATR-FTIR allows for direct analysis by probing the evanescent field at the interface between a high refractive index crystal and the sample. Micro-FTIR couples FTIR with microscopy, producing tens-of-micrometer-scale chemical maps of zoning, mineral assemblages, and alteration in thin sections and polished mounts, while reflectance and DRIFT (diffuse reflectance infrared Fourier transform) configurations extend FTIR to rough surfaces and powders. Because vibrational frequencies depend on bond strength

* Definitions of terms presented in **blue** are given in the glossary on page 81.

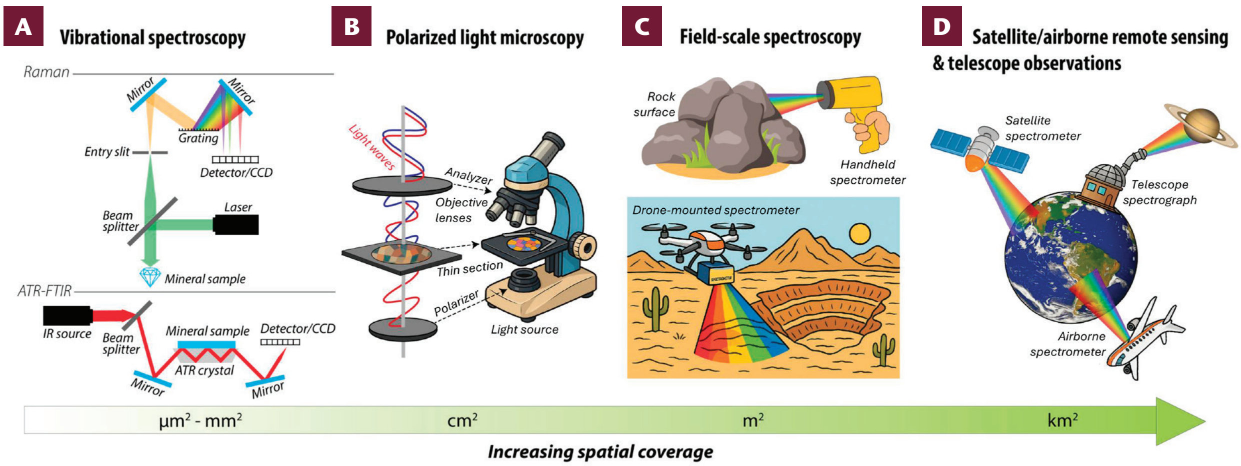

Figure 1 Select light-based spectroscopic techniques used to characterize minerals across increasing spatial scales. (**A**) Vibrational spectroscopy methods, such as Raman spectroscopy and attenuated total reflectance (ATR) with Fourier Transform Infrared (FTIR) spectroscopy, probe molecular vibrations at scales of approximately μm^2 to mm^2. Schematic shows common hardware elements used in optical spectrometers, including a source, beam splitter, grating, mirror/optics, and a detector. (**B**) Polarized light microscopy analyzes mineral optical properties in petrographic thin sections, typically covering spatial areas on the order of cm^2. (**C**) Field-scale spectroscopy and remote sensing, using handheld or drone-mounted instruments, allows mineral identification across m^2-scale outcrops. (**D**) Satellite imagery and telescope observations enable reflectance spectroscopy at planetary to global scales (tens to thousands of km^2), supporting large-area compositional mapping. Elements of some graphics were supported by DALL-E and free vector art from https://vectorportal.com/.

and reduced mass, band positions and widths can be used to quantify cation substitution, hydrogen bonding, and structural disorder within mineral lattices.

Raman spectroscopy provides a complementary view of vibrational modes and is particularly powerful for phase identification, assessing crystallinity, and detecting polymorphs or structural disorder. Raman maps and images are used to trace reaction fronts, exsolution textures, and deformation fabrics. Micro-Raman enables measurements on individual grains and inclusions that are difficult to probe by other methods. Variants such as confocal, imaging, polarized Raman, and surface-enhanced Raman spectroscopy (SERS) further improve spatial resolution, mapping capability, and sensitivity. Fluorescence, however, can interfere with Raman measurements, often overwhelming weak vibrational signals and obscuring mineral peaks. To address this challenge, time-gated Raman reduces fluorescence by rejecting long-lived emission, while shifted excitation Raman difference spectroscopy (SERDS) collects spectra at two closely spaced laser wavelengths and subtracts them, removing the fluorescence background while amplifying Raman peaks.

These principles are illustrated by the mineral assemblage shown in Figure 2, where spectral differences arise directly from contrasts in bonding and crystal structure among olivine, serpentine, and magnetite. In olivine, the FTIR spectrum is dominated by strong Si-O stretching absorptions near ~850–1000 cm^{-1}, while the Raman spectrum shows a characteristic doublet near ~820–860 cm^{-1} corresponding to symmetric stretching of isolated SiO_4 tetrahedra. The position and separation of this doublet shift systematically with Fe–Mg substitution. Serpentine exhibits prominent Si-O features around ~900 cm^{-1} and OH stretching absorptions near ~3600 cm^{-1} in FTIR, and Si-O lattice modes between ~300–800 cm^{-1} in Raman, consistent with its layered structure and hydrogen bonding. Magnetite's FTIR spectrum is dominated by relatively broad Fe-O lattice modes due to high symmetry, mixed Fe^{2+}–Fe^{3+} valence, and electron-phonon coupling, while its Raman spectrum is characterized by a distinct Fe-O mode near ~660 cm^{-1} typical of the spinel structure. In conventional Raman spectroscopy, these vibrational features may be overwhelmed by fluorescence, which produces a broad background signal, whereas SERDS isolates the Raman peaks by suppressing this background. The combined "whole rock" spectrum illustrates how overlapping contributions from these distinct bonding environments produce composite spectral features, underscoring the need to interpret peaks in the context of crystal chemistry rather than position alone.

Minerals subjected to depth record Earth's interior conditions through structural and compositional changes, and their inclusions preserve the pressure, temperature, and fluid chemistry at entrapment. Vibrational spectroscopy identifies these inclusions and their volatile species while constraining redox conditions, volatile budgets, and host-rock evolution. Diamonds are especially useful because they form at great depths and trap high-pressure phases rarely preserved at the surface. Raman and FTIR measurements reveal inclusion composition, structural state, and phase transitions such as exsolution or breakdown during ascent (e.g., Smith et al. 2022). Combined with major and trace element data and, when available, crystallographic information, these observations constrain mantle composition, pressure and temperature conditions, redox state, and the transport of deep material to the surface.

In laboratory experiments that replicate deep Earth conditions, vibrational spectroscopy provides direct, in situ constraints on crystal structure, bonding, and phase stability (e.g., Johnston et al. 2002). Raman spectra track pressure- and temperature-driven changes in lattice vibrations, including systematic frequency shifts, band splitting, and intensity changes that reflect compression, symmetry changes, cation ordering, or phase transitions. In diamond anvil cell studies, a laser is focused through one anvil onto the micrometer-scale sample, and the backscattered signal is collected along the same optical path, enabling real-time monitoring of structural evolution within the confined sample volume, while pressure is independently determined from the calibrated shift of ruby fluorescence lines under compression.

Complementing these measurements of bond vibrations and structural transitions, light scattering can also be used to probe elastic properties through Brillouin spectroscopy. In this technique, monochromatic visible laser light,

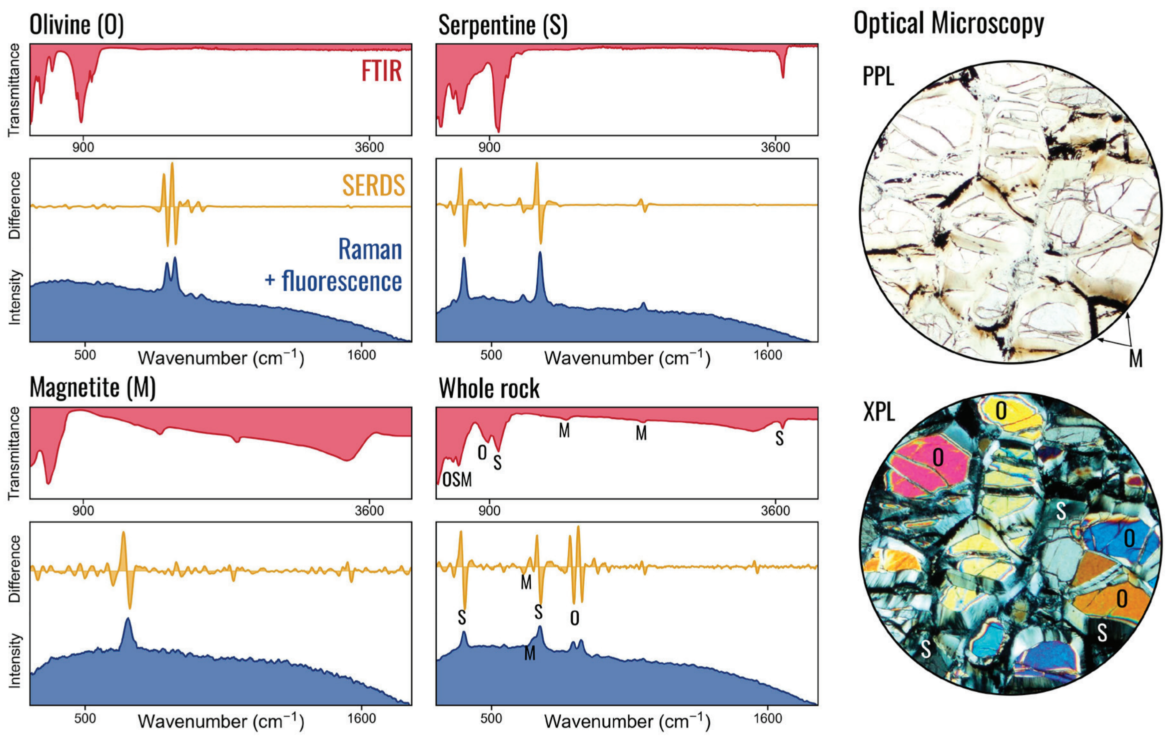

Figure 2 Spectroscopic and optical characterization of a serpentinized lherzolite composed of olivine (O), serpentine (S), and magnetite (M). FTIR spectra show characteristic vibrational absorptions for each mineral, with data sourced from the RRUFF database (Lafuente et al. 2015). Raman spectra display both mineral-specific vibrational modes and the fluorescent background, which is typically removed during preprocessing. SERDS removes this background by subtracting two slightly shifted spectra. The "whole rock" spectra are synthetic 1:1:1 sums of the three mineral spectra for illustrative purposes and do not represent actual abundances. Optical microscopy images in plane-polarized light (PPL) and cross-polarized light (XPL) show the distribution of O, S, and M in thin section. Raman and SERDS data provided by Miraterra Technologies. FTIR data from the RRUFF Project. Optical images © Alessandro Da Mommio – www.alexstrekeisen.it.

commonly 532 or 514 nm, is inelastically scattered by thermally excited acoustic phonons, producing a small frequency shift proportional to the velocity of sound in the crystal (e.g., Sinogeikin and Bass 2000). Because acoustic wave velocities depend on elastic stiffness, Brillouin measurements on single crystals provide direct access to **elastic moduli**. When combined with density measurements and crystallographic orientation, these data constrain the full elastic tensor, linking lattice-scale bonding to **macroscopic** mechanical properties. Brillouin spectroscopy is therefore widely used in mineral physics to determine single-crystal elastic constants at ambient and high-pressure conditions, complementing Raman and FTIR measurements of vibrational structure and phase stability.

Together, vibrational and Brillouin spectroscopies connect atomic-scale bonding, phase transitions, and elastic properties, allowing light-based methods to probe both the structural and mechanical behavior of minerals across a range of pressure and temperature conditions.

Electronic Fingerprints: UV-Vis-NIR Spectra of Minerals

UV-Vis-NIR spectroscopy probes electronic transitions and higher-order vibrational features that complement the bond-specific information obtained from FTIR and Raman spectroscopy. Whereas vibrational spectroscopy measures quantized atomic motions, UV-Vis-NIR spectroscopy primarily detects transitions between electronic energy levels. These absorptions are sensitive to oxidation state, coordination environment, site symmetry, and crystal chemistry, making them powerful indicators of mineral composition and structure. Measurements can be collected on powders, thin sections, polished grains, and bulk samples at laboratory and field scales.

Absorptions arise from several distinct processes. **Crystal field transitions** occur when surrounding anions split the otherwise degenerate energy levels of *d*-orbitals in transition metals such as Fe, Mn, or Cr. The electrostatic field created by neighboring ions lifts this degeneracy, producing distinct energy levels whose separations depend on coordination geometry and bond length (e.g., Rossman 1975). **Charge transfer transitions** involve electron movement between a ligand and a cation or between neighboring cations, typically generating strong, broad absorptions in the ultraviolet and visible regions, as in iron oxides. Intervalence charge transfer between Fe^{2+} and Fe^{3+} produces diagnostic near-infrared features that directly reflect redox conditions.

Defect-related absorptions arise from structural imperfections or **radiation** damage that introduce localized electronic states within the band structure. These color centers are responsible for the coloration of minerals, such as fluorite and smoky quartz, and record radiation history and defect populations (Rossman 1996). In addition, overtone and combination bands of fundamental vibrational modes appear in the near infrared and shortwave infrared (SWIR), linking UV-Vis-NIR measurements directly to the bonding environments identified in mid-infrared spectroscopy.

In mineral physics, UV-Vis-NIR spectroscopy constrains electronic structure under increasing pressure and temperature. Because crystal field splitting depends on bond length and coordination, shifts in band position and intensity track compression, cation ordering, and site distortion. Under high pressure, spectral changes reveal spin transitions and coordination changes in minerals such as ferropericlase, bridgmanite, and garnet, providing insight into density, elasticity, and radiative heat transport in Earth's interior.

The same electronic absorptions observed in laboratory samples are used to interpret field, airborne, and satellite reflectance spectra. Bands associated with Fe-bearing silicates, oxides, clays, and carbonates allow mineral assemblages and alteration patterns to be mapped from outcrop to planetary scale. By linking electronic transitions to crystal chemistry, UV-Vis-NIR spectroscopy provides a common framework for interpreting mineral properties across spatial scales.

Minerals in Thin Section: Optical Microscopy

Optical microscopy is one of the oldest and most widely used light-based techniques in mineral analysis and typically operates at centimeter-scale fields of view. In its simplest form, bright-field microscopy uses transmitted or reflected light to examine the morphology, grain size, color, and textural relationships of minerals. These observations establish grain boundaries, inclusions, and reaction textures that provide essential geological context.

Polarized light microscopy adds a physical dimension to these observations by exploiting the anisotropic optical properties of crystals. In anisotropic minerals, the refractive index depends on crystallographic direction. When plane-polarized light enters such a crystal, it splits into two rays that travel at different velocities and vibrate in perpendicular planes. This velocity difference produces a phase shift between the rays as they exit the crystal. When analyzed between crossed polarizers, the phase shift generates interference colors that depend on birefringence, thickness, and orientation.

Birefringence arises because different crystallographic directions respond differently to the electric field of incident light, producing differences between principal refractive indices that reflect crystal symmetry and bonding anisotropy. As a result, interference colors and extinction behavior provide diagnostic information about mineral identity and crystallographic orientation. In practice, plane-polarized light reveals color, pleochroism, and relief, allowing assessment of absorption behavior, grain boundaries, and refractive index contrast relative to adjacent phases, whereas cross-polarized light shows interference colors arising from birefringence, as well as extinction angles, twinning, and crystallographic orientation through changes in intensity and color during stage rotation.

A strength of optical microscopy is its ability to place mineral spectra and compositions into a clear textural and spatial context. In Figure 2, the distribution of olivine, serpentine, and magnetite in thin section is readily distinguished by differences in color, birefringence, and opacity. Magnetite is opaque in plane-polarized light and remains black under crossed polars. Olivine displays high second- to third-order interference colors in cross-polarized light due to its relatively high birefringence. Serpentine exhibits lower first-order interference colors and a characteristic fibrous texture in cross-polarized light, reflecting its sheet silicate structure and hydration during serpentinization. These petrographic observations guide interpretation of the accompanying FTIR and Raman spectra by identifying which phases contribute to specific spectral features and by revealing reaction relationships such as serpentinization textures or oxide formation along grain boundaries.

ROCKS IN THE WILD: FIELD-SCALE SPECTROSCOPY

Point and Shoot Spectra: Field Exploration of Igneous and Metamorphic Rocks

At outcrop and hand-sample scales, field spectroscopy bridges laboratory measurements and larger airborne or satellite observations. Portable UV-Vis-NIR and Raman spectrometers are increasingly used to characterize the mineralogy of igneous and metamorphic rocks directly on outcrops, boulders, and drill cores. Most handheld Vis-NIR-SWIR spectrometers operate over approximately 0.35 to 2.5 μm and measure reflected sunlight or instrument-generated illumination. The resulting reflectance spectra record the same diagnostic electronic and overtone absorption features described at laboratory scales, but integrated over millimeter- to centimeter-scale spot sizes.

In igneous terrains, field reflectance spectra collected along traverses or across individual outcrops are used to map variations in mineral assemblages and alteration intensity. Absorption bands associated with Fe^{2+} crystal field transitions in olivine and pyroxene, Fe^{3+} charge transfer in oxides, and combination bands of hydrous minerals allow rapid discrimination of lithologic units and alteration zones. These spectral signatures help distinguish primary magmatic domains from hydrothermal overprints and delineate reaction halos around veins, dikes, and breccia bodies.

In metamorphic settings, field-based UV-Vis-NIR spectra track changes in mineral composition and redox state across gradients in pressure, temperature, and deformation. Systematic variations in band depth and position in Fe-bearing silicates and oxides reflect changes in site occupancy, oxidation state, and reaction progress. When collected along structural transects or across mapped isograds, these spectra provide quantitative constraints that complement petrographic observations, especially where fine grain size or weathering obscures optical textures.

Measurements on drill core extend this approach into the subsurface. Spot measurements or automated scanning of core surfaces provide continuous mineralogical profiles that support unit correlation and alteration mapping. Because field spectra are influenced by illumination geometry, surface roughness, weathering rinds, and mineral mixing within the instrument footprint, they are typically interpreted in conjunction with laboratory reference libraries and selected samples analyzed in detail. Even so, the ability to collect dense, spatially explicit measurements at the outcrop links thin-section petrography and laboratory spectra to meter-scale geological structures.

Field and laboratory spectroscopy also provide controlled systems for observing mineral reactions as they occur. Geological carbon mineralization offers a clear example. When CO_2 reacts with silicate minerals such as olivine or serpentine, primary silicates transform into carbonates and secondary phases. These transformations produce systematic spectral changes, including growth of carbonate CO_3^{2-} bands and shifts in Si-O and OH features as structures reorganize. FTIR and Raman measurements therefore record the progression from reactant to product phases and constrain reaction pathways, intermediate assemblages, and the extent of conversion.

EARTH FROM ABOVE: AIRBORNE IMAGING SPECTROSCOPY

Hovering for Spectra: Drone Surveys

Imaging spectrometers mounted on low-altitude platforms such as drones bridge the gap between point field measurements and regional airborne surveys. Centimeter- to meter-scale pixels resolve individual outcrops, rock faces, waste rock piles, and alteration zones while preserving spatial continuity in diagnostic absorption features. Each pixel records a reflectance spectrum, that is, the ratio of reflected to incident radiation as a function of wavelength, capturing the same electronic transitions and vibrational overtone and combination bands described at laboratory and handheld scales.

Drone-based systems typically operate in the visible to shortwave infrared range and measure bidirectional reflectance of solar radiation under defined illumination and viewing geometries. Absorption band depth and shape

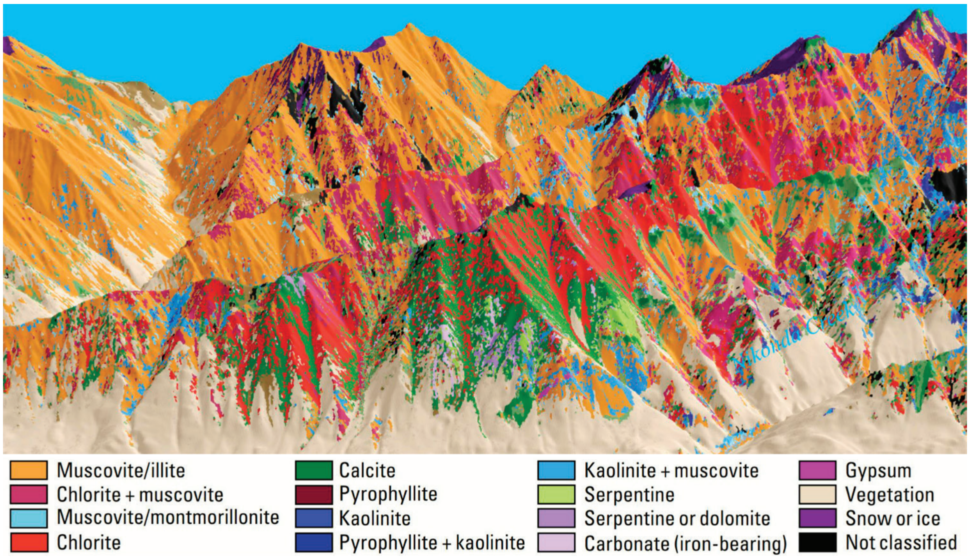

FIGURE 3 Airborne hyperspectral mineral map of the Orange Hill area in Alaska's Wrangell-St. Elias National Park and Preserve (USA), draped over a digital elevation model. Colors correspond to spectral classes representing minerals such as muscovite, chlorite, serpentine, calcite, and gypsum. MODIFIED FROM THE UNITED STATES GEOLOGICAL SURVEY.

depend not only on intrinsic mineral properties but also on optical path length, grain size, surface roughness, and porosity. In coarse crystalline rocks, photons may cross multiple grain boundaries, increasing path length and strengthening absorption features, whereas in fine-grained or weathered materials, scattering and surface coatings can reduce band contrast and alter spectral slopes.

Because flight altitudes are low, drone surveys achieve higher spatial resolution than conventional airborne systems while covering substantially larger areas than ground measurements. These capabilities are illustrated in the airborne hyperspectral mineral map of the Orange Hill area in Alaska's Wrangell-St. Elias National Park and Preserve (FIG. 3). Visible to shortwave infrared mineral classes draped over a digital elevation model reveal muscovite-rich zones relevant to copper exploration and delineate alteration halos and weathering patterns across steep terrain. The mineral classes are defined by specific absorption features associated with Al-OH, Fe-bearing silicates, carbonates, and other phases, directly reflecting the bonding environments described at laboratory scales.

At this intermediate scale, reflectance spectra commonly represent mixtures of multiple minerals within each pixel. The observed signal may approximate a linear combination of endmember spectra in coarse mixtures, but intimate mixing and multiple scattering introduce nonlinear effects. Radiative transfer models and comparison with laboratory reference spectra help separate compositional variations from illumination and surface effects. By extending laboratory-defined absorption physics across entire outcrops and terrains, drone imaging spectroscopy links thin-section observations, handheld measurements, and larger airborne and satellite datasets.

WORLDS FROM AFAR: SATELLITE AND TELESCOPIC SPECTROSCOPY

Orbital Spectroscopy of Terrestrial Bodies in the Inner Solar System

Satellite-based imaging spectrometers and multispectral sensors acquire spatially resolved reflectance and, in some cases, thermal emission spectra of planetary surfaces at spatial scales from tens of meters to kilometers. In reflected-light measurements, instruments record the wavelength-dependent ratio of reflected to incident solar radiation. In thermal infrared measurements, they detect emitted radiation governed by surface temperature and wavelength-dependent emissivity. Both approaches rely on the same fundamental absorption processes described at laboratory scales, but integrated over larger spatial footprints and influenced by illumination geometry, surface roughness, and, where present, atmospheric absorption.

Recent spaceborne imaging spectrometers, such as PRISMA, EnMAP, and EMIT, provide contiguous spectral coverage across hundreds of bands, enabling mineralogical mapping at regional to global scales (e.g., van der Meer et al. 2012; Bishop et al. 2020; Portela et al. 2025). These datasets extend airborne mineral mapping to the planetary scale, capturing diagnostic absorption features associated with crystal field transitions, charge transfer processes, and vibrational overtones in clays, carbonates, iron oxides, and silicates. Atmospheric correction and radiometric calibration are required to isolate surface reflectance from scattering and absorption by gases and aerosols, ensuring that retrieved spectra can be directly compared to laboratory reference measurements.

On airless bodies such as the Moon, reflectance spectra primarily record surface mineralogy modified by space weathering and grain size effects. Thermal infrared spectroscopy has been used to map silicate composition by measuring reststrahlen bands and Christiansen features, revealing a globally anorthositic crust and basaltic mare deposits (e.g., Greenhagen et al. 2010). Near-infrared reflectance measurements have also detected OH and H_2O absorption features in surface materials, especially at high latitudes (Pieters et al. 2009), indicating bound or implanted volatiles.

On Mars, visible to shortwave infrared imaging spectrometers, such as OMEGA and CRISM, detect absorption bands associated with Fe-bearing silicates, phyllosilicates, sulfates, carbonates, and hydrated silica (e.g., Carter et al. 2013; Ehlmann and Edwards 2014). These features arise from Fe^{2+} crystal field transitions and OH and H_2O vibrational overtones, allowing identification of alteration minerals formed through water-rock interaction. The depth, position, and shape of these bands provide constraints on mineral composition, hydration state, and, in some cases, crystallinity. Combined with in situ rover measurements, orbital spectra reveal a record of aqueous alteration, redox evolution, and sedimentary processes across Mars' crust (e.g., Scheller et al. 2021, 2022).

On Venus and Mercury, dense atmospheres or extreme temperatures limit spectral windows, but near-infrared observations through atmospheric transmission bands and visible-near infrared measurements from orbit have provided constraints on surface composition, including basaltic volcanism and variations in Fe-bearing phases (Helbert et al. 2015; Nittler and Weider 2019). In all cases, interpretation depends on comparing orbital spectra to laboratory measurements collected under controlled grain size, temperature, and viewing geometries.

Across **terrestrial bodies**, orbital spectroscopy extends laboratory-defined absorption physics to planetary scales. Crystal field transitions, charge transfer bands, and vibrational overtones measured in thin sections and powders form the reference framework for interpreting reflectance and emission spectra acquired from orbit. By accounting for illumination geometry, temperature, atmospheric effects, and spectral mixing within large pixels, these methods allow mineralogical and geochemical processes to be inferred across entire planetary surfaces.

Orbital and Flyby Spectroscopy of Outer Solar System Moons and Small Bodies

Spectroscopy of icy moons and small bodies in the outer Solar System relies primarily on reflectance measurements in the near- and mid-infrared, where vibrational modes of H_2O, CO_2, CO, CH_4, NH_3, and related species produce strong absorption features. Because these bodies are cold, thermal emission is often weak in the near infrared, and observed spectra are dominated by reflected sunlight modulated by surface composition, grain size, temperature, and radiation processing. The positions, widths, and shapes of ice absorption bands depend on crystal structure, phase (crystalline versus amorphous), temperature, and chemical environment, making them sensitive probes of both composition and physical state.

Crystalline and amorphous water ice, for example, exhibit distinct band shapes and substructure in the 1.5-, 2.0-, and 3.0-µm regions. Radiation damage from charged particles and micrometeorite impacts can amorphize ice, broaden absorption bands, and generate new spectral features associated with radiolytic products. Salts and hydrates modify band positions and continuum slopes through changes in bonding environment and scattering behavior. As a result, reflectance spectra encode not only mineralogy but also the balance between endogenic resurfacing and exogenic irradiation.

On Jupiter's ocean-bearing moons Europa and Ganymede, spectroscopy from *Galileo* and *Juno* has identified absorption features consistent with hydrated salts, sulfuric acid hydrate, and other radiation products at the surface (e.g., Carlson et al. 2009; Tosi et al. 2024). These features likely reflect a combination of ocean-derived materials transported upward and chemical modification driven by intense magnetospheric irradiation. Band depth variations and spatial correlations with geologic features provide constraints on exchange between subsurface reservoirs and the irradiated surface layer.

In the Saturn system, infrared spectra from *Cassini* revealed water-ice-dominated surfaces with compositional heterogeneity tied to active processes. On Enceladus, spectral signatures of fresh, crystalline water ice in eruptive plume deposits contrast with more processed terrains, indicating ongoing resurfacing (Jaumann et al. 2008). The same features appear in plume-derived particles in Saturn's E-ring and on neighboring moons, showing how reflectance spectroscopy traces material transport and surface modification across a planetary system (Hendrix et al. 2018).

Across outer Solar System bodies, orbital and flyby spectroscopy thus links vibrational absorption physics to surface temperature, phase state, irradiation history, and geologic exchange processes. As in the inner Solar System, laboratory spectra collected under controlled temperature and radiation conditions provide the reference framework for interpreting remotely sensed data, allowing compositional and physical evolution to be inferred at planetary scales.

Telescopic Spectroscopy of Planetary Surfaces and Small Bodies

Spectroscopic observations with ground- and space-based telescopes are an important technique for studying the surfaces of planets, moons, and small bodies. By combining spectral and spatial information, telescopic observations complement orbital and in situ measurements, extend coverage to targets not visited by spacecraft, and provide temporal monitoring over seasonal and decadal timescales. For example, spectroscopy from facilities like the *Hubble Space Telescope* and *James Webb Space Telescope* has identified sodium chloride (via color centers) on Europa (Trumbo et al. 2019) and revealed connections between Ganymede's polar surface ice and CO_2 exosphere (Bockelée-Morvan et al. 2024).

Telescopic observations have also revealed that spectral signatures of water ice also pervade the major moons of Uranus and Neptune, as well as objects comprising the distant Kuiper Belt, and most of these satellites and small bodies also exhibit near-infrared signatures of at least one more-volatile ice, like CO_2, CO, CH_4, or N_2 (Brown 2012; Clark et al. 2013). The composition and abundances of these other ices provide important constraints on both the formation conditions and volatile-loss history of each body.

Continued near- and mid-infrared observations from space- and ground-based telescopes refine constraints on the composition, thermal properties, and evolution of outer Solar System bodies. Time series spectroscopy of atmospheres, plumes, and surfaces tracks changes in volatile distributions and active processes.

Linking Satellite and Telescopic Spectra to Meteorites and Analog Samples

Spectroscopy allows researchers to compare laboratory measurements of meteorites with reflectance and emission spectra obtained from telescopes and spacecraft. Meteorites retain mineral and chemical records of early Solar System processes, and their well characterized spectra provide reference points for interpreting remotely sensed surfaces. This linkage is the basis for assigning meteorites to parent bodies and for reconstructing the alteration, space weathering, and thermal histories of small bodies and planets.

Spectroscopic analyses of meteorites, combined with structural and chemical studies, characterize their mineralogy, textures, and alteration history and provide a framework for assigning them to petrologic and chemical classes. Vibrational spectroscopy has long been used to connect meteorite compositions to remotely sensed planetary spectra, including early work on Martian meteorites (Hamilton et al. 1997; Wang et al. 2004). Telescopic and spacecraft observations reveal diagnostic reflectance and emission spectra for asteroid populations, which are organized into spectral classes such as S, C, X, and V types defined by their visible to near infrared reflectance characteristics. Laboratory spectra of meteorites, collected under controlled viewing geometry and grain size, are compared directly to these asteroid spectra to infer surface mineralogy and possible meteorite analogs (e.g., Young et al. 2022). Classic examples include linking Vesta to the howardite-eucrite-diogenite suite of basaltic achondrites, associating many S-type asteroids with space-weathered ordinary chondrites, and relating Ceres and other C-type asteroids to carbonaceous chondrite–like compositions (e.g., Ehlmann et al. 2018).

These spectral links are refined by accounting for space weathering, grain size, and temperature, and are increasingly tested by sample return missions that enable direct comparison of returned regolith spectra with pre-encounter telescopic and spacecraft data. Such comparisons calibrate meteorite analogs and support identification of new minerals in meteorites, expanding the range of recognized phases and improving interpretation of unresolved spectral features on asteroid and planetary surfaces.

CONCLUDING REMARKS

Light-based spectroscopy has been used extensively in Earth and planetary sciences and provides quick, non-destructive ways to obtain mineral compositions, structures, and physical properties. Improvements in detector sensitivity, optical stability, and compact instrument design now support routine use in core logging, mine environments, rover operations, and high-pressure experiments. These developments have broadened the range of pressure, temperature, and compositional conditions that can be measured and strengthened the link between laboratory spectra and observations collected in the field and from orbit.

Looking forward, spectroscopy will continue to play a central role in mineral physics, geology, and planetary science through improved instrument stability and sensitivity, broader use of robotic and drone platforms, and closer integration with airborne and satellite observations. UV-Vis-IR instruments on upcoming missions to the Moon, Mars, and the outer Solar System will detect hydrated minerals, salts, organics, and ices relevant to planetary evolution and habitability. Combined with machine learning tools for automated interpretation, spectroscopy will continue to connect atomic-scale bonding and elasticity to planetary-scale mineral mapping, improving our ability to characterize Earth's interior and planetary surfaces across spatial scales.

ACKNOWLEDGMENTS

We thank Wendy Calvin, Kam Bhowany, and Ginger Brown for their thoughtful and constructive reviews. We thank Alessandro Da Mommio for optical microscopy images, Miraterra Technologies for Raman and SERDS spectra, the RRUFF Project for FTIR spectra, and Arca Climate Technologies for discussions on carbon mineralization.

REFERENCES

Bishop JL, Bell JF III, Moersch JE (2020) Remote Compositional Analysis: Techniques for Understanding Spectroscopy, Mineralogy, and Geochemistry of Planetary Surfaces. Cambridge University Press, 652 pp

Bockelée-Morvan D and 27 coauthors (2024) A patchy CO_2 exosphere on Ganymede revealed by the *James Webb* Space Telescope. Astronomy & Astrophysics 690: L11, doi: 10.1051/0004-6361/202451599

Brown ME (2012) The compositions of Kuiper Belt objects. Annual Review of Earth and Planetary Sciences 40: 467-494, doi: 10.1146/annurev-earth-042711-105352

Carlson RW and 7 coauthors (2009) Europa's surface composition. In: Pappalardo RT, McKinnon WB, Khurana KK (eds) Europa. University of Arizona Press, Tucson, pp 283-327

Carter J, Poulet F, Bibring JP, Mangold N, Murchie S (2013) Hydrous minerals on Mars as seen by the CRISM and OMEGA imaging spectrometers: updated global view. Journal of Geophysical Research: Planets 118: 831-858, doi: 10.1029/2012JE004145

Clark RN, Carlson R, Grundy W, Noll K (2013) Observed ices in the Solar System. In: Gudipati M, Castillo-Rogez J (eds) The Science of Solar System Ices. Springer, New York, pp 3-46, doi: 10.1007/978-1-4614-3076-6_1

Ehlmann BL, Edwards CS (2014) Mineralogy of the Martian surface. Annual Review of Earth and Planetary Sciences 42: 291-315, doi: 10.1146/annurev-earth-060313-055024

Ehlmann BL and 6 coauthors (2018) Ambient and cold-temperature infrared spectra and XRD patterns of ammoniated phyllosilicates and carbonaceous chondrite meteorites relevant to Ceres and other Solar System bodies. Meteoritics & Planetary Science 53: 1884-1901, doi: 10.1111/maps.13103

Greenhagen BT and 12 coauthors (2010) Global silicate mineralogy of the Moon from the Diviner lunar radiometer. Science 329: 1507-1509, doi: 10.1126/science.1192196

Hamilton VE, Christensen PR, McSween HY Jr (1997) Determination of Martian meteorite lithologies and mineralogies using vibrational spectroscopy. Journal of Geophysical Research: Planets 102: 25593-25603, doi: 10.1029/97JE01874

Helbert J, Müller N, Hashimoto GL (2015) Venus surface composition constrained by observation and experiment. Space Science Reviews 214: 1-33

Hendrix AR and 5 coauthors (2018) Surface composition of Saturn's icy moons. In: Schenk PM, Clark RN, Howett CJA, Verbiscer AJ, Waite JH (eds) Enceladus and the Icy Moons of Saturn. University of Arizona Press, Tucson, pp 307-322

Jaumann R and 18 coauthors (2008) Distribution of icy particles across Enceladus' surface as derived from Cassini-VIMS measurements. Icarus 193: 407-419, doi: 10.1016/j.icarus.2007.09.013

Johnston CT and 5 coauthors (2002) Novel pressure-induced phase transformations in hydrous layered materials. Geophysical Research Letters 29: 17-1-17-4, doi: 10.1029/2002GL015402

King PL, Mernagh TP (2024) A review of infrared and Raman spectroscopy in the geosciences. In: Anbar A, Weis D (eds) Treatise on Geochemistry, Volume 8 (Third Edition). Elsevier, Amsterdam, pp 723-787, doi: 10.1016/B978-0-323-99762-1.00093-0

Lafuente B, Downs RT, Yang H, Stone N (2015) The power of databases: the RRUFF project. In: Armbruster T, Danisi RM (eds) Highlights in Mineralogical Crystallography. De Gruyter, Berlin, pp 1-30, doi: 10.1515/9783110417104-003

Nittler LR, Weider SZ (2019) The surface composition of Mercury. Elements 15: 333-338, doi: 10.2138/gselements.15.1.33

Portela B, van der Werff H, Hecker C, van der Meijde M (2025) Characterising mineral chemistry variation as a proxy for fluid composition using EMIT spaceborne hyperspectral data. Ore Geology Reviews 182: 106673, doi: 10.1016/j.oregeorev.2025.106673

Pieters CM and 28 coauthors (2009) Character and spatial distribution of OH/H_2O on the surface of the Moon seen by M^3 on Chandrayaan-1. Science 326: 568-572, doi: 10.1126/science.1178658

Rossman GR (1975) Spectroscopic methods in mineralogy. Reviews in Mineralogy 3: 1-26

Rossman GR (1996) Color in minerals. American Mineralogist 81: 1-11

Scheller EL, Ehlmann BL, Hu R, Adams DJ, Yung YL (2021) Long-term drying of Mars by sequestration of ocean-scale volumes of water in the crust. Science 372: 1075-1081, doi: 10.1126/science.abc7717

Scheller EL and 65 coauthors (2022) Aqueous alteration processes in Jezero crater, Mars—implications for organic geochemistry. Science 378: 1105-1110, doi: 10.1126/science.abo5204

Sinogeikin SV, Bass JD (2000) Single-crystal elasticity of mantle minerals at high pressure by Brillouin spectroscopy. Reviews in Mineralogy and Geochemistry 41: 371-409

Smith EM, Krebs MY, Genzel PT, Brenker FE (2022) Raman identification of inclusions in diamond. Reviews in Mineralogy and Geochemistry 88: 451-473, doi: 10.2138/rmg.2022.88.08

Tosi F and 27 coauthors (2024) Salts and organics on Ganymede's surface observed by the JIRAM spectrometer onboard Juno. Nature Astronomy 8: 82-93, doi: 10.1038/s41550-023-02107-5

Trumbo SK, Brown ME, Hand KP (2019) Sodium chloride on the surface of Europa. Science Advances 5: eaaw7123, doi: 10.1126/sciadv.aaw7123

van der Meer FD and 9 coauthors (2012) Multi- and hyperspectral geologic remote sensing: a review. International Journal of Applied Earth Observation and Geoinformation 14: 112-128, doi: 10.1016/j.jag.2011.08.002

Wang A, Kuebler K, Jolliff B, Haskin LA (2004) Mineralogy of a Martian meteorite as determined by Raman spectroscopy. Journal of Raman Spectroscopy 35: 504-514, doi: 10.1002/jrs.1175

Young JM and 7 coauthors (2022) Nano-FTIR investigation of the CM chondrite Allan Hills 83100. Journal of Geophysical Research: Planets 127: e2021JE007166, doi: 10.1029/2021JE007166 ■